INTERNATIONAL JOURNAL OF CLIMATOLOGY
Int. J. Climatol. (in press)
Published online in Wiley InterScience
(www.interscience.wiley.com) DOI: 10.1002/joc.1396

NEAR-SURFACE-TEMPERATURE LAPSE RATES ON THE PRINCE OF WALES ICEFIELD, ELLESMERE ISLAND, CANADA: IMPLICATIONS FOR REGIONAL DOWNSCALING OF TEMPERATURE

SHAWN J. MARSHALL,[a,*] MARTIN J. SHARP,[b] DAVID O. BURGESS[b] and FARON S. ANSLOW[a]
[a] *Department of Geography, University of Calgary, Calgary AB, Canada*
[b] *Department of Earth and Atmospheric Sciences, University of Alberta, Edmonton AB, Canada*

Received 2 May 2005
Revised 14 March 2006
Accepted 4 July 2006

ABSTRACT

Screen temperatures were monitored from May 2001 to April 2003 in an array of 25 sites on the Prince of Wales Icefield, Ellesmere Island, Canada. The observational network covered an area of *ca* 15 650 km^2 and spanned an altitude ranging from 130 to 2010 m above sea level. The spatial array provides a record of near-surface-temperature lapse rates and mesoscale temperature variability on the icefield. The mean daily lapse rate in the 2-year record is $-4.1\,^{\circ}$C km^{-1}, with an average summer lapse rate of $-4.3\,^{\circ}$C km^{-1}. Surface-temperature lapse rates in the region are therefore systematically less than the free-air lapse rates that are typically adopted for extrapolations of sea-level temperature to higher altitudes. Steep lapse rates, resembling moist adiabatic rates in the free air (-6 to $-7\,^{\circ}$C km^{-1}), are more common in summer at our site and are associated with enhanced cyclonic activity (low-pressure and high relative vorticity) and southerly flow aloft. In contrast, northerly, anticyclonic flow prevails when summer lapse rates are weak (above $-2\,^{\circ}$C km^{-1}). The low surface-temperature lapse rates and their systematic synoptic variability have important implications for applications that require downscaling or extrapolation of surface- or boundary-layer temperatures, such as modelling of glacier mass balance. We illustrate this in an analysis of observed *versus* modelled snowmelt on the icefield. Copyright © 2006 Royal Meteorological Society.

KEY WORDS: climate downscaling; lapse rates; glacier mass balance; surface energy balance; Canadian Arctic; mountain climatology

1. INTRODUCTION

Spatial-temporal patterns of temperature variability are relevant to a broad range of Earth surface processes, and many scientific disciplines confront the need to estimate local- or regional-scale surface temperatures based on point measurements or atmospheric models. These two approaches can be summarized as follows: (1) extrapolation of temperatures from meteorological stations, which are concentrated at low elevations and are sparse in many regions of the world, or (2) interpolation of temperatures from reanalyzed climatology, operational forecast, or climate models, with grid-cell resolutions from 10s to 100s of km. For instance, climate change impact studies at local or regional scales require downscaling of modelled temperatures to the site or region of interest (Leung and Wigmosta, 1999).

Temperature is considered to be a relatively straightforward meteorological variable to extrapolate or interpolate on climatic time scales, because temperature fields are continuous and horizontal temperature gradients are typically low for long-term climatology, in which the effects of weather systems and fronts average out. Vertical temperature gradients are much higher, and the common practice when extrapolating temperature fields to higher or lower elevations is to assume a constant atmospheric lapse rate of -6 to

* Correspondence to: Shawn J. Marshall, Department of Geography, University of Calgary, 2500 University Drive NW, Calgary AB, T2N 1N4, Canada; e-mail: shawn.marshall@ucalgary.ca

Copyright © 2006 Royal Meteorological Society

$-7\,^{\circ}\mathrm{C\ km^{-1}}$ (Legates and Willmott, 1990; Walland and Simmonds, 1996; Pollard and Thompson, 1997; Glover, 1999). This choice is based on average observed lapse rates in the free atmosphere, and represents a typical moist adiabatic cooling rate (Seidel and Free, 2003).

Despite their broad application, it is not clear that free-air lapse rates offer an appropriate estimate of vertical gradients in surface temperature. Local surface energy balance (net radiative and turbulent heat flux) is the primary determinant of surface temperatures. This introduces the complicated role of the surface environment (albedo, roughness, topographic aspect, and wind regime) and atmospheric conditions (clouds, relative humidity, synoptic flow) in dictating spatial and temporal patterns of surface temperature (McCutchan, 1983; Greuell and Böhm, 1998; Pepin *et al.*, 1999). Elevation still exacts many influences, as incoming shortwave and longwave radiation increases and decreases with altitude, respectively. In addition, sensible and latent heat transfers depend on atmospheric temperature and moisture content, which exhibit strong vertical gradients in the free atmosphere. High-altitude surface environments are therefore still influenced by free-atmosphere temperature gradients, but they are subject to additional controls.

We examine near-surface temperature patterns in this paper, as recorded by shielded temperature sensors located 0.5 to 2 m above the surface. We refer to the measured vertical temperature gradients as near-surface or screen-temperature lapse rates. Few published studies address screen-temperature lapse rates and their variability, although their complexity is well acknowledged (Pielke and Mehring, 1977; Richner and Phillips, 1984; Tabony, 1985; McCutchan and Fox, 1986; Greuell and Böhm, 1998; Bolstad *et al.*, 1998; Pepin *et al.*, 1999; Pepin, 2000). Regional and local studies that report screen-temperature lapse rates typically find average values that are less than free-air lapse rates: for instance $-5.3\,^{\circ}\mathrm{C\ km^{-1}}$ in Iceland (Jóhannesson *et al.*, 1995), $-5.5\,^{\circ}\mathrm{C\ km^{-1}}$ in the Færoe Islands (Humlum and Christiansen, 1998), $-5.2\,^{\circ}\mathrm{C\ km^{-1}}$ in the Argentinian Andes (Trombotto *et al.*, 1997), and $-5.2\,^{\circ}\mathrm{C\ km^{-1}}$ in the Canadian Rockies (Shea *et al.*, 2004).

Pepin and Losleben (2002) present an excellent discussion and comparison of near-surface *versus* free-air lapse rates in the eastern slopes of the Colorado Rocky mountains. Screen-temperature lapse rates exhibit diurnal and seasonal variability, with significant departures from nearby free-air lapse rates. In addition to the radiative influences that are manifest in the diurnal and seasonal variability, Pepin and Losleben (2002) demonstrate the presence of synoptic-scale influences on near-surface lapse rates in the Colorado front ranges. Pepin *et al.* (1999) identified similar local- and synoptic-scale controls on screen-temperature lapse rate in the British uplands.

The studies above span up to 2000 m of elevation, and offer some guidance for extrapolation of temperatures from valley-bottom weather stations to those at higher altitudes in mountain environments. This is of interest in many applications, including assessment of the signature and impacts of climate change at high altitudes (Giorgi *et al.*, 1997; Fyfe and Flato, 1999). Screen-temperature lapse rates are also critical in the estimation of alpine glacier mass balance and the response of glacial systems to climate change (Braithwaite and Olesen, 1989; Reeh, 1991; Jóhannesson *et al.*, 1995; Arnold *et al.*, 1996; Zuo and Oerlemans, 1997; Huybrechts and de Wolde, 1999). This application is the focus of our long-term field and modelling studies, and the remainder of this paper examines screen-temperature lapse rates in a glacierized environment.

Long-term meteorological data from glaciers and icefields is scant, but available meteorological data suggest that screen-temperature lapse rates are less than the typical free-air values (*ca* $-7\,^{\circ}\mathrm{C\ km^{-1}}$) that are commonly adopted in glacier mass balance and ice sheet modelling. Braun and Hock (2004) report the frequent occurrence of shallow and inverse lapse rates over a melting surface on King George Island, Antarctica. Consistent with this, mean monthly lapse rates measured by M.J.Sharp varied from $+0.5$ to $-3.5\,^{\circ}\mathrm{C\ km^{-1}}$ in a six-year record from three meteorological stations spanning 922 m of altitude on the John Evans Glacier, Ellesmere Island (unpublished data). There is a pronounced seasonal cycle in this data with persistent inversions giving rise to weak lapse rates in the winter months. Stronger temperature gradients prevail in the summer.

Greuell and Böhm (1998) discuss the complexity of screen-temperature lapse rates on melting glacier surfaces and their dependence on boundary-layer processes. A melting snow or ice surface will be held at $0\,^{\circ}\mathrm{C}$, suppressing warming of the lower boundary layer and acting to reduce vertical temperature gradients over glaciers and icefields in the summer. The high solar reflectivity of snow surfaces also dramatically alters the local energy balance compared with lower altitude snow-free sites in the glacier ablation zone or off the icefield (e.g. in a glacier forefield or valley-bottom environment). For this reason, screen-temperature lapse

Copyright © 2006 Royal Meteorological Society

DOI: 10.1002/joc

rates measured from the snow-free site to the upper reaches of the ice mass will not be the same as those measured at two or more sites on the glacier. These environmental influences need to be considered in mass balance studies that are driven by observed station data, which is generally recorded off-glacier and at lower altitude.

In the study reported here, we installed a network of 25 temperature loggers over an 1880-m range of elevation on a high Arctic icefield, maintaining a relatively homogeneous surface environment (snow or, in the summer melt season at the lowest altitudes, exposed glacial ice). The observational network spanned an area of 15 650 km^2, so we consider the meteorological observations to be regional in scale. The study ran for 2 years, providing a temperature record that illustrates a rich variability of daily, monthly, and seasonal surface-temperature lapse rates. This paper presents the 2-year record and an initial interpretation of the synoptic controls of the observed lapse-rate variability.

2. FIELD SITE AND METHODS

Air temperature, snow accumulation, and annual mass balance measurements were collected for the period from April 2001 to May 2003 on the Prince of Wales (POW) Icefield, Ellesmere Island, Nunavut, Canada (Figures 1, 2). The icefield descends to sea level on the east coast of Ellesmere Island and it terminates terrestrially on the western margin at altitudes from 400 to 600 m above sea level. Nunataks and snow-covered hills protrude to altitudes above 2000 m at several locations. There are significant environmental differences on the western and eastern flanks of the icefield. The western outlets of the glacier give way to snow-free tundra through the summer months, which is subject to significant radiative warming. Smith Sound and northern Baffin Bay lie east of the icefield. The seasonal cycle of sea ice and open-water conditions in this region is complicated by the presence of the North Water polynya, a large seasonal open-water feature that may be a significant source of sensible heat and moisture for the icefield in late winter and spring (Barber *et al*., 2001). We shall return to the potential impact of the North Water polynya later. In addition to the North Water, complex local winds are observed in Smith Sound owing to strong cold air outbreaks that are channelled through Nares Strait (e.g. Samelson *et al*., 2006). These may also influence coastal sites on the eastern flanks of the icefield.

The observational network consists of two transects that span the icefield, one in the north (the NPOW line) and one in the south (the SPOW line). The NPOW line was established in April 2001 and is 166 km in length, with altitudes ranging from 130 m on the eastern margin to 2010 m at the highest point (site POWHI, denoted PH in Figure 2). The northeastern transect runs along the Leffert Glacier, a major outlet of the icefield. The western portion of the NPOW line descends to 610 m altitude on the northwestern margin. Temperature sensors on the NPOW transect were in place until May 2003. The 131-km long SPOW line was established in May 2002 and also descends to the ice margins on the eastern and western sides of the icefield. The southern ice divide, the highest elevation of the SPOW line, is at 1350 m altitude (POWSTH in Figure 2). Ten sites were instrumented along this transect. The eastern transect follows a major glacier outlet system that was unofficially named the *Koerner Glacier*, with our lowest observation site positioned about 5 km from the Baffin Bay coast, at an altitude of 180 m. The western portion of the SPOW transect terminates at an altitude of 450 m on the southwestern ice margin. Travel on the icefield was by snowmobile, with Twin Otter access and all other field logistics supported by the Polar Continental Shelf Project, Canada.

Screen-level temperatures at each site in Figure 2 were recorded at 30-min intervals using a combination of HOBO H8-PRO temperature loggers (from Onset Scientific Ltd.) and SP2000 temperature–relative humidity loggers (from Veriteq Instruments Inc.). All sensors were deployed in Onset radiation shields and were mounted on poles hand-augured into the ice. Instruments were mounted at a height of 1 to 1.5 m above the snowpack. All sites were in open environments with little or no influence from topographic shading. Instrument locations were representative of the prevailing topographic slope and aspect in that sector of the icefield; local depressions were avoided. Plastic (PVC) poles that were used in 2001–2002 flexed under the weight of the instruments, leading to unexpected burial and loss of some instruments. All the instruments

Copyright © 2006 Royal Meteorological Society

DOI: 10.1002/joc

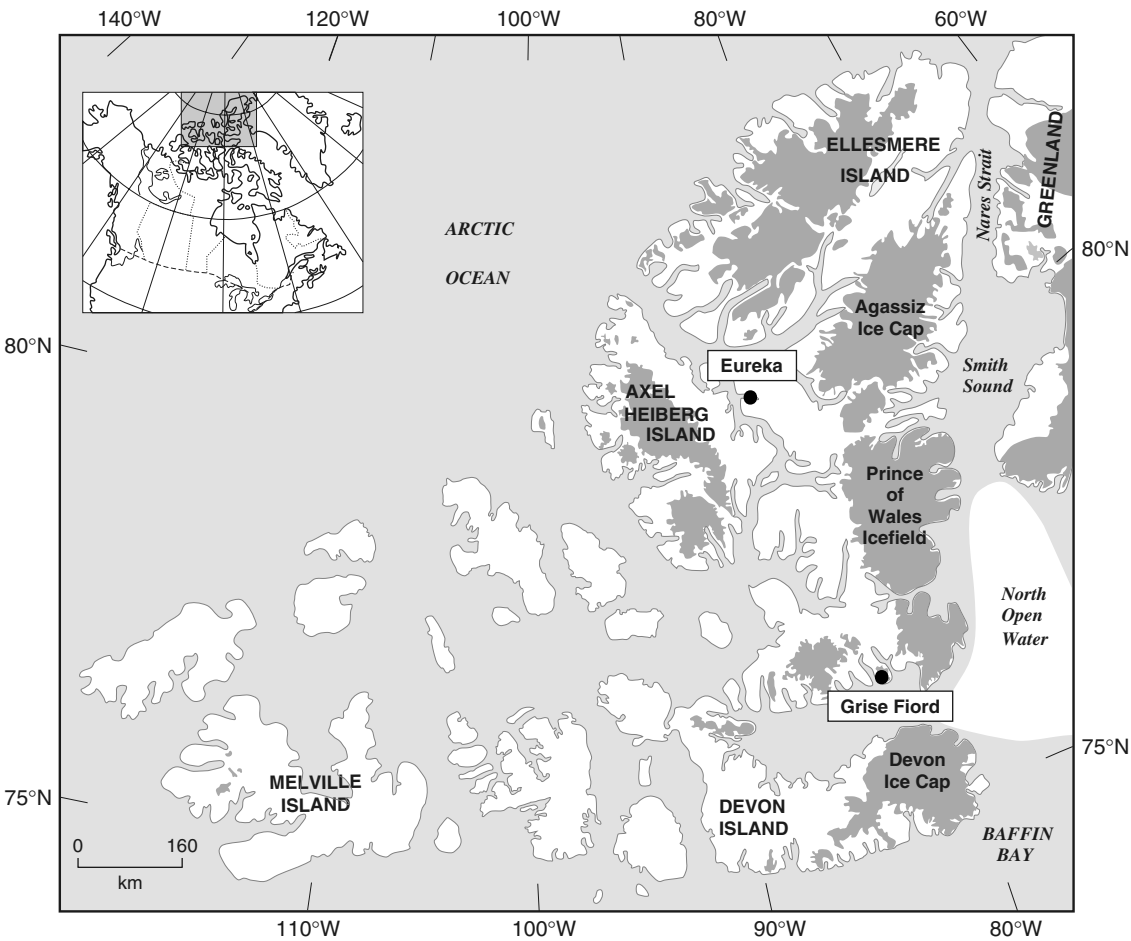

Figure 1. Location of the Prince of Wales Icefield, Ellesmere Island, Nunavut, Canada. Grise Fiord and Eureka are the nearest available weather stations of the Meteorological Service of Canada

were replaced using 10-foot steel poles in spring 2002 and data recovery was much improved in 2002–2003 (23 of 25 stations recovered).

Instrument accuracy of the manufacturer is assessed to be 0.8 °C at −30 °C and 0.2 °C at 0 °C. Temperature sensors were calibrated through comparison with control data from a shielded, ventilated temperature gauge at the University of Calgary weather research station. Sensors were set up in the weather station compound at 2-m height and measurements were made at 5-min intervals over a 1- to 2-week calibration period. The average offset over the calibration period was calculated relative to the control instrument. There was no systematic drift of instruments, but we measured offsets from 0.1 to 0.7 °C. Uncertainties in the calibration arise owing to (1) performance of the sensors at very cold temperatures, which were not represented in the calibration, and (2) effects of varying distances above the ground in the field. Taking this error to be up to 1 °C for the persistent cold temperatures at the field site, and assuming instrument offsets of as much as 0.7 °C, we estimate the uncertainty in the temperature data to be 1.2 °C.

We have also undertaken control experiments to test the effect of height above the ground for a suite of 20 sensors deployed at 10-cm intervals ranging from 10 to 200 cm in height. These studies were carried out for a period of 2 months over snow and grass surfaces. We conclude from these studies (unpublished data) that temperature gradients in the near-surface boundary layer are largely confined to the region from 0 to 50 cm above the surface. Above 50 cm, mean daily temperatures were within 0.1 °C of the 2-m height data. Sensors deployed from 20 to 50 cm were within 0.2 °C of the 2-m measurements, but with systematic diurnal errors

Copyright © 2006 Royal Meteorological Society

DOI: 10.1002/joc

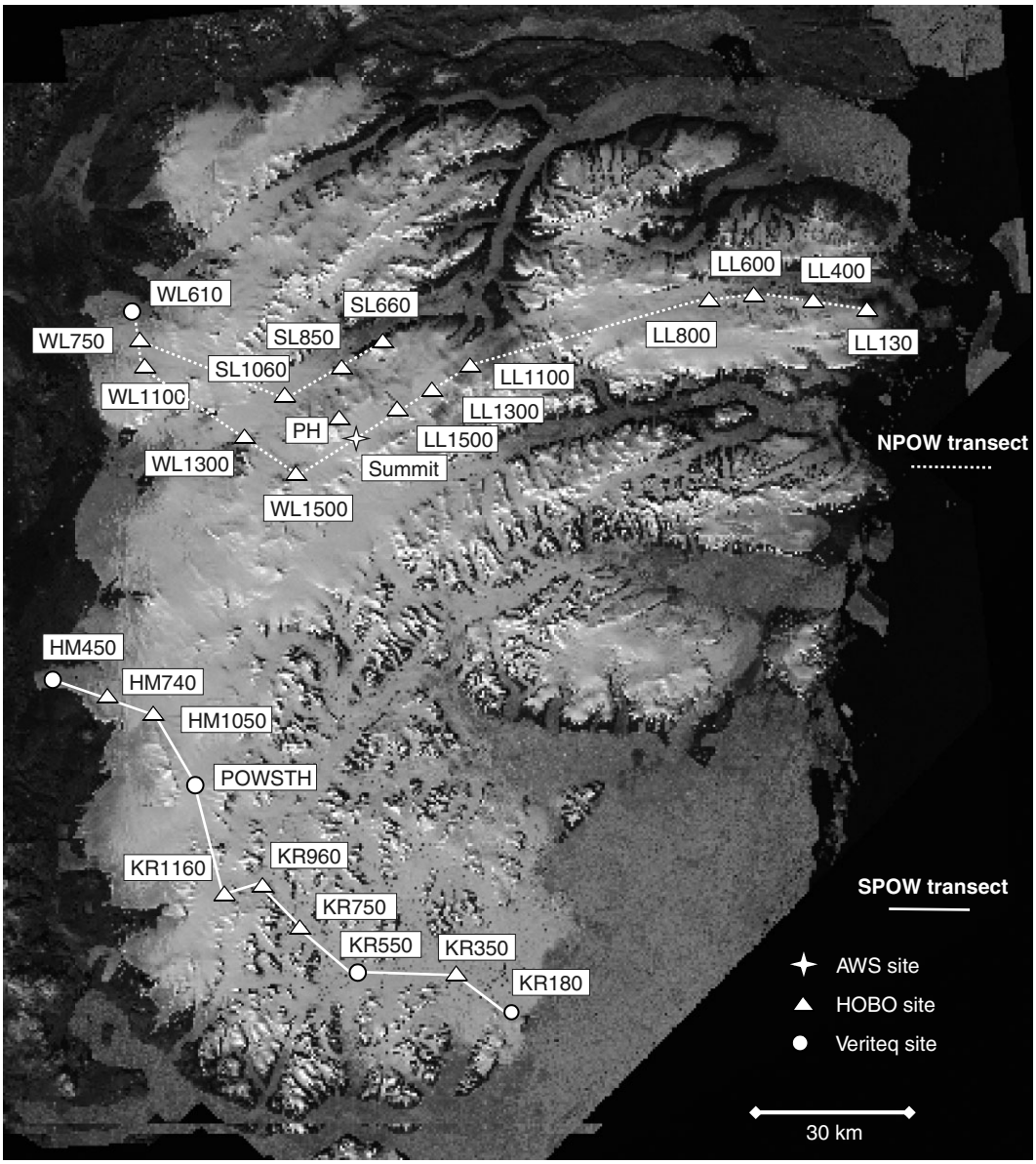

Figure 2. Temperature monitoring sites on the Prince of Wales Icefield, 2001–2003. The automatic weather station site is marked with a star, HOBO temperature datalogger sites are marked with triangles, and Veriteq temperature/relative humidity monitoring sites are marked with circles

of up to 1.5 °C (warmer by day and cooler by night). These biases compensate in the daily averages. To minimize these effects, we restrict our analysis to daily and monthly average temperatures and to data from sensors at heights above 50 cm. The depth of the lower boundary layer that appears problematic −50 cm in our study – will vary with winds and surface environment (roughness, albedo), so this needs to be evaluated more fully (Greuell and Böhm, 1998).

In addition to the HOBO and Veriteq loggers, an automatic weather station (AWS) was in place at the summit site (1730 m) for the duration of the study. Hourly wind, radiation, snow depth, temperature, relative humidity, and air pressure data were recorded at the AWS from May to December in 2001 and May to October in 2002, with loss of battery power in the winter months.

Copyright © 2006 Royal Meteorological Society

DOI: 10.1002/joc

The location and altitude of all sites are provided in Table I, along with the period for which each sensor was operational. Position estimates are based on surveying by handheld GPS. Estimated vertical GPS accuracy is 10 m.

3. RESULTS: TEMPERATURE DATA

Temperature data from each site were processed to construct minimum, mean, and maximum daily temperatures, as well as the standard deviation in daily temperature, on the basis of 30-min data. If a sensor was found partially buried or to have fallen over, we omit all data from the time when it was found to be immersed or resting on the snow/ice surface. The time of such an occurrence is readily apparent in the daily temperature data because the range and standard deviation in the daily temperature cycle gets strongly muted. In addition to fallen or partially buried sensors, we excluded March and April data from any instrument that was within 30 cm of the snow surface at the time of data recovery (April or early May of each year).

We had good data coverage for the summer months: 13 sites in 2001 and 21 sites in 2002. Instrument burial and battery losses led to less complete coverage in winter and spring months. Because of the more complete record available for 2002–2003, much of the analysis focuses on this year. Table II summarizes daily temperature statistics for 2002–2003 from all of the icefield sites. Mean annual temperatures and average

Table I. Temperature monitoring sites on the Prince of Wales Icefield, Ellesmere Island, Canada, May 2001–April 2003

Site	Latitude (deg : min)	Longitude (deg : min)	Elevation (m)	Data record duration
North transect, 2001–2003				
WL610	78°43.418′N	81°11.945′W	610	2002/2005–2003/2004
WL750	78°42.644′N	81°13.832′W	747	2001/2005–2002/2002; 2002/2005–2003/2004
SL850	78°38.354′N	79°31.765′W	850	2001/2005–2003/2004
SL1060	78°35.929′N	79°51.506′W	1060	2001/2005–2001/2012; 2002/2005–2002/2006
WL1100	78°38.549′N	81°12.102′W	1094	2002/2005–2003/2004
WL1300	78°29.932′N	80°13.619′W	1310	2001/2005–2003/2004
WL1500	78°27.241′N	79°54.955′W	1500	Not recovered (buried)
SUMMIT	78°29.120′N	79°25.643′W	1727	2001/2005–2002/2001; 2002/2005–2002/2009
POWHI	78°29.761′N	79°36.555′W	2009	2001/2005–2003/2004
LL1500	78°33.022′N	79°04.069′W	1510	2002/2005–2003/2004
LL1300	78°36.394′N	78°40.223′W	1308	2001/2005–2003/2004
LL1100	78°37.860′N	78°28.414′W	1105	2001/2005–2002/2003; 2002/2005–2003/2004
LL800	78°42.844′N	76°21.642′W	799	2001/2005–2001/2010
LL600	78°43.038′N	75°58.511′W	602	2001/2005–2001/10; 2002/2005–2003/2004
LL400	78°41.967′N	75°28.257′W	395	2001/2005–2001/2010; 2002/2005–2003/2004
LL130	78°40.617′N	74°58.160′W	129	2001/2005–2002/2001; 2002/2005–2002/2009
South transect, 2002–2003				
HM450	78°04.749′N	81°53.309′W	450	2002/2005–2003/2004
HM740	78°03.060′N	81°38.896′W	740	2002/2005–2002/2009
HM1050	78°01.514′N	81°15.230′W	1056	2002/2005–2003/2004
POWSTH	77°52.266′N	80°48.639′W	1350	2002/2005–2003/2004
KR1160	77°42.480′N	80°34.062′W	1160	Not recovered (buried)
KR960	77°42.858′N	80°14.997′W	960	2002/2005–2003/2004
KR750	77°38.448′N	79°59.835′W	750	2002/2005–2002/2012
KR550	77°31.629′N	79°32.397′W	550	2002/2005–2003/2004
KR350	77°31.680′N	78°44.812′W	350	2002/2005–2002/2010
KR180	77°27.443′N	78°15.823′W	175	Not recovered (melted out & buried)

Copyright © 2006 Royal Meteorological Society

DOI: 10.1002/joc

Table II. Prince of Wales Icefield daily temperature data, 2002–2003. T_{min} and T_{max} refer to minimum and maximum daily average temperatures over the year, from May 1, 2002 to April 30, 2003. $\overline{T}_a$ is the average annual temperature, $\overline{\sigma}_d$ and ΔT_d are the average standard deviation and range in daily temperatures, and *PDD* refers to the net annual positive degree days, an index of the heat available for snow and ice melt

Site	T_{min}(°C)	T_{max}(°C)	$\overline{T}_a$ (°C)	$\overline{\sigma}_d$ (°C)	ΔT_d (°C)	PDD (°C·d)
LL130		5.76				127.0
LL400	−34.89	4.80	−13.84	1.82	6.79	112.2
LL600	−37.92	3.52	−15.23	2.13	7.91	80.0
LL1100	−42.45	3.03	−18.40	2.14	7.96	28.0
LL1300	−41.80	1.54	−18.41	2.08	7.69	13.0
LL1500	−44.31	0.69	−20.90	2.09	7.24	2.9
SUMMIT		−0.98				1.0
POWHI	−37.75	−2.30	−19.07	1.32	4.51	0.0
WL1300	−39.30	3.75	−18.63	1.80	6.77	10.6
WL1100	−38.55	1.74	−17.33	1.90	7.06	21.8
SL850	−43.01	4.47	−18.23	2.14	7.99	44.1
WL750	−38.27	4.83	−15.72	1.56	6.00	107.1
WL610	−41.91	6.78	−15.72	1.50	5.45	213.3
KR350		2.50				50.1
KR550	−41.62	2.89	−17.15	1.95	6.72	53.9
KR750		2.97		2.14	7.94	53.6
KR950	−41.27	3.17	−17.39	2.46	9.01	32.4
POWSTH	−42.94	0.71	−20.55	1.76	5.91	7.2
HM1050	−40.28	2.67	−17.75	1.96	7.19	15.0
HM750		2.51				47.9
HM450	−41.73	5.66	−15.19	1.39	5.14	166.6

annual measures of temperature variability (standard deviation and range of daily temperatures) are presented for the 16 sites with complete and reliable year-round data.

The annual cycle of mean daily near-surface temperatures was generally coherent. For instance, sites LL400 and LL1500, which are 102 km apart, were correlated at $r = 0.98$. Continuous screen-temperature lapse rates could be constructed from each pair of stations such as this, but we chose to analyze all stations on the icefield simultaneously to give a regional-scale measure of daily lapse rates. This also reduces the influence of the effects of instrument height and local meteorological conditions at a particular site, which may produce unrepresentative lapse rates. For instance, cold air drainage or warm air advection from the proglacial environment may impact some lower sites more than others. We see evidence of potential influences of cold air drainage on the Stygge Glacier sites, SL850 and SL1050, but these sites did not strongly influence the full icefield elevation–temperature regressions. Pervasive local temperature inversions were not observed at any other lower site.

Systematic local temperature anomalies were observed at site POWHI (PH in Figure 2), the uppermost station in the grid. Mean annual temperatures at POWHI in 2002–2003 were 1.8 °C warmer than at site LL1500. Analysis of daily data from site POWHI shows that there are no significant departures from vertical temperature gradients observed at all other sites on the icefield during summer months, but POWHI appears to be thermally isolated from the main icefield plateau from October to May. POWHI is systematically warmer during this period, with minimum winter temperatures at this site being above those measured at LL1500 by 6.6 °C. Temperature variability is also anomalously low at this site.

Further study is needed to confirm that the POWHI data is valid; it was the only sensor that operated year-round in this portion of the icefield. Free-air processes and the persistent winter inversions that are characteristic of polar regions may genuinely have more influence here. The site is on a nunatak above the main icefield plateau, and high winds at the site may disrupt inversions that setup at lower altitudes in

Copyright © 2006 Royal Meteorological Society

DOI: 10.1002/joc

winter months. Additional meteorological observations are needed to evaluate this. To be conservative in our interpretations, we omit this site from the lapse-rate calculations in this paper.

4. MEAN DAILY LAPSE RATES

Mean daily screen-temperature lapse rates were calculated through a simple linear regression of daily average temperature *versus* altitude for all available stations. With site POWHI excluded, an elevation range of 1600 m was sampled by the array. Mean daily lapse rates were calculated for the entire 2-year period from May 1, 2001 to April 30, 2003. The regression results are plotted in Figure 3, which is a 2-year record of mean daily lapse rates, $\beta(t)$. There is a great deal of variability in lapse rates on daily and weekly time scales, as well as a marked seasonal cycle in the data. The mean daily lapse rate for the full data set was $-3.7\,^{\circ}\mathrm{C\ km^{-1}}$. Stronger lapse rates prevail in the summer months, with an average JJA value of $-4.3\,^{\circ}\mathrm{C\ km^{-1}}$ for the two summers (*cf* Table III). In general, strong linear elevation–temperature relationships are found when lapse rates are steep ($\beta < -5\,^{\circ}\mathrm{C\ km^{-1}}$), and weak lapse rates ($\beta > -2\,^{\circ}\mathrm{C\ km^{-1}}$) have low R^2 values and weak or no statistical significance. The variability in daily lapse rates is high: an average standard deviation of 2.4 °C for the 2-year record. The standard deviation in summer (JJA) is 1.7 °C.

Average daily temperatures for each site on the icefield are plotted in Figure 4(a) and (b) for June 9 and June 27, 2002, two days with contrasting screen-temperature lapse rates. The June 9 example has a near-surface lapse rate of $-6.8\,^{\circ}\mathrm{C\ km^{-1}}$ and a linear vertical temperature gradient over the entire region ($R^2 = 0.96$), while the lapse rate shallows to $-2.4\,^{\circ}\mathrm{C\ km^{-1}}$ on June 27, with a weak linear relationship ($R^2 = 0.27$). These two days represent extremes of lapse rates for summer 2002 and can be related to contrasting synoptic conditions (Section 4). The regression in Figure 4(b) is statistically significant ($p < 0.05$), but the scatter in

Table III. Mean monthly and seasonal lapse rates. Columns 1 and 2 are based on a regression of all available stations on the icefield for 2001–2002 and 2002–2003. Columns 3 and 4 represent subsets of the data for the northern and eastern sites ($n = 12$ in each case)

	$\overline{\beta}$(°C km^{-1})			
	01–02	02–03	02–03 (N)	02–03 (E)
May	−3.6	−4.5	−3.9	−3.9
June	−4.2	−5.4	−5.8	−5.7
July	−3.4	−5.1	−5.3	−4.6
August	−3.4	−4.6	−4.8	−4.0
September	−3.3	−4.8	−4.9	−4.3
October	−4.8	−4.2	−4.4	−3.3
November	−3.3	−6.0	−6.7	−5.5
December	−2.3	−5.1	−5.6	−6.3
January	−0.5	−5.5	−5.5	−6.1
February	−1.5	−4.0	−4.4	−5.1
March	−1.1	−3.1	−3.8	−5.4
April	−1.2	−3.5	−5.2	−6.0
Summer (JJA)	−3.7	−5.0	−5.3	−4.8
Autumn (SON)	−3.8	−5.1	−5.3	−4.4
Winter (DJF)	−1.6	−4.8	−5.2	−5.8
Spring (MAM)	−2.0	−3.5	−4.3	−5.1
Annual mean	−2.8	−4.6	−5.0	−5.0
Standard deviation	2.7	2.2	2.3	2.4

Copyright © 2006 Royal Meteorological Society

DOI: 10.1002/joc

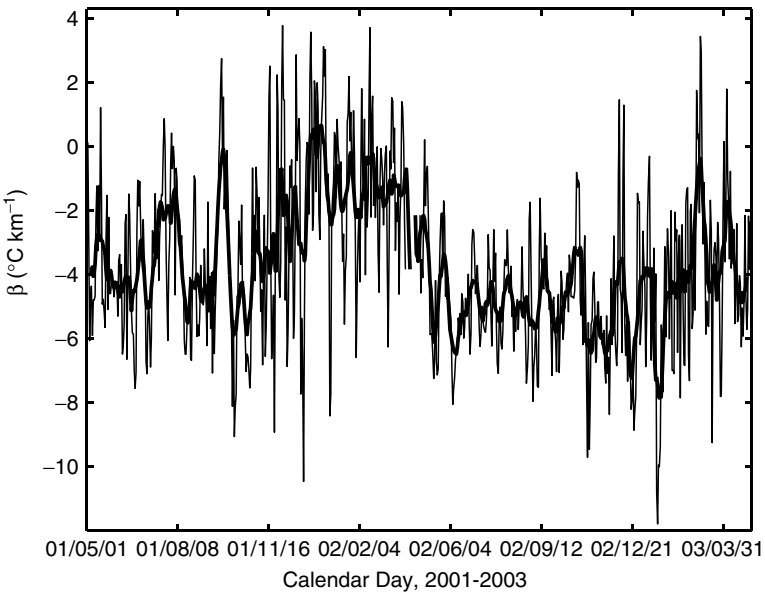

Figure 3. Mean daily surface-temperature lapse rate over the icefield for the period from May 1, 2001 to April 30, 2003. Lapse rates are calculated from regressions of daily average temperature *versus* elevation at all available icefield stations. The heavy line is a 9-day moving average

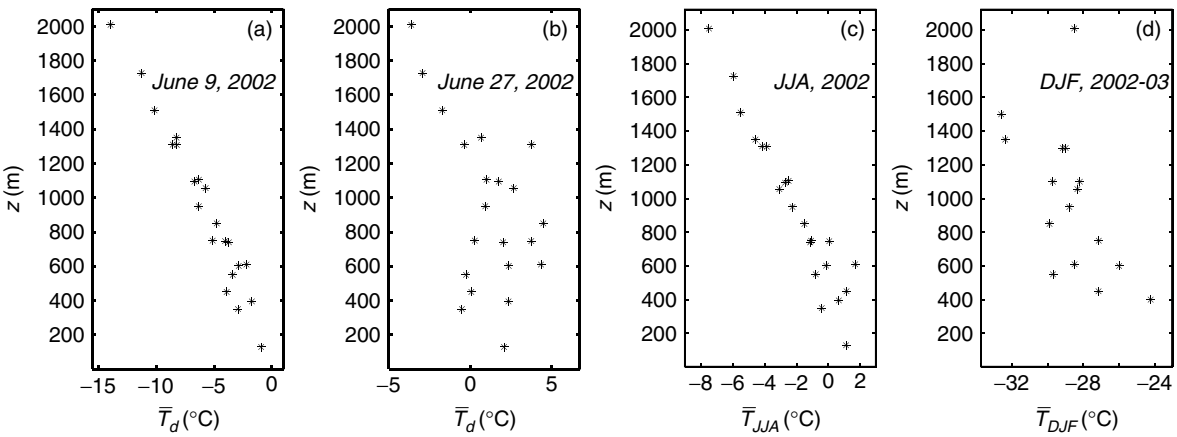

Figure 4. Temperature *versus* elevation for all available temperature stations on the icefield. (a) and (b) depict mean daily temperature on June 9 and June 27, 2002. These two days illustrate strong and weak linear elevation–temperature relationships ($-6.8\,^{\circ}$C km^{-1} and $-2.4\,^{\circ}$C km^{-1}, respectively). (c) and (d) show mean seasonal temperatures in summer (JJA) 2002 and winter (DJF) 2002–2003

the temperature data is evident, indicating isothermal conditions or a weak inversion below 1400 m and a return to cooling at altitudes above this height.

Figure 4(c) and (d) plots mean summer (JJA) and mean winter (DJF) temperatures at all available stations in 2002–2003. The mean seasonal lapse rates in each case are $-5.0\,^{\circ}$C km^{-1} and $-4.8\,^{\circ}$C km^{-1} with the upper site (POWHI) excluded ($-5.1\,^{\circ}$C km^{-1} and $-4.5\,^{\circ}$C km^{-1} when the site is included in the regression). The correlation between temperature and altitude is extremely strong for average summer temperatures: $r = -0.96$. In winter months, frequent inversions weaken the temperature–altitude relationship, but it remains strong $r = -0.75$, or $r = -0.81$ with POWHI included. The strength and significance of the regression is higher for the seasonal fit to the data when daily variability is averaged out.

Copyright © 2006 Royal Meteorological Society

DOI: 10.1002/joc

Table III compiles monthly, seasonal, and annual mean lapse rates for the entire data set, with the 2001–2002 and 2002–2003 observation years reported separately. Mean annual lapse rates in 2002–2003 were 1.8 °C km^{-1} steeper than those in 2001–2002, with the difference reflected in all seasons. Despite monthly differences and steeper lapse rates in 2002–2003, the annual cycle is consistent in the two observation years. There were minimal stations operating on the icefield through winter and spring 2001–2002, but data recovery was good for the summer months, so we are confident that the interannual differences in the summer data, −5.0 °C km^{-1} in 2002 and −3.7 °C km^{-1} in 2001, are genuine.

The first year of observation sampled only the northern icefield transect, and it is not clear *a priori* that daily lapse rates in the southern transect should reflect those in the north. To test the validity of this comparison, we analyzed the 2002–2003 data from the northern and southern transects separately. The third set of data in Table III presents lapse-rate statistics from the 2002–2003 NPOW transect for direct comparison with those of 2001–2002. The systematic differences between the two observation years persist, with the northern subset of the data within 0.4 °C km^{-1} of the icefield average. It appears that (1) there were genuine differences between these years, and (2) the northern and southern sectors of the Prince of Wales Icefield experience similar mean daily lapse rates, suggesting regional- or synoptic-scale (rather than local) controls.

The overall pattern of daily lapse-rate variability was also broadly similar on the eastern *versus* western sides of the icefield (column 4 of Table III), despite the different environments (marine *vs* terrestrial margins). There are, however, systematic differences in mean winter and spring lapse rates on the eastern flanks. The average December to May lapse rate for the eastern sites was −5.5 °C km^{-1} in 2002–2003, compared with −4.2 °C km^{-1} for the full data set. The difference for June through November was only 0.4 °C km^{-1} and was opposite in sign. This systematic seasonal difference is consistent with the potential role of the North Water polynya in providing a source of sensible heat to the lower regions of the eastern margin of the icefield. Shallow convective instability that is associated with the North Water may also play a role in disrupting the shallow thermal inversions that otherwise occur in the winter months. By contrast, the western margins are prone to inversions in winter months, but the pattern is reversed in summer, with radiative heat generating steeper summer lapse rates on the western flanks of the icefield.

5. SYNOPTIC ANALYSES

Daily NCEP 700-mb and 500-mb height fields (Kalnay *et al.*, 1996) were examined to characterize mean atmospheric flow in the region of the Prince of Wales Icefield for the period 1950–2003, and the subset of data from May 2001 to April 2003 was compared in detail with the observed near-surface lapse rates. NCEP fields were attained from the NOAA-CIRES Climate Diagnostics Center, Boulder, Colorado (http://www.cdc.noaa.gov). We characterized daily 500-mb geostrophic flow fields over the icefield using geopotential height gradients centered on the 2.5° NCEP grid-cell that is most closely associated with the site, (80 °W, 77.5 °N). Daily and monthly 500-mb flow indices were derived following the method of Losleben *et al.* (2000).

5.1. Calculation of flow indices

Barotropic pressure systems prevail over the Prince of Wales Icefield, with low pressures at all atmospheric levels when the polar vortex extends over the Canadian Arctic Archipelago or during passage of cold-core cyclones through the region (Hare, 1968; Alt, 1987; Serreze, 1995). Anticyclonic ridging that can influence the region in summer months is also vertically stacked. This is evident in the high correlation between the daily NCEP 700-mb and 500-mb heights ($r = 0.97$) as well as the daily mean surface pressures recorded at the POWN site ($r = 0.96$, for the 14 months that are available in the 2001–2003 observation period). The strong correlation with the surface pressure data indicates that 500- and 700-mb pressures are likely to be well-represented in the NCEP Reanalysis.

Assuming a geostrophic balance, upper-level winds can be estimated from the 500-mb geopotential height gradients. For zonal wind speed u, meridional wind speed v, gravitational acceleration g, Coriolis parameter

Copyright © 2006 Royal Meteorological Society

DOI: 10.1002/joc

f, and 500-mb heights Z (λ, θ),

$$u = -\frac{g}{fR}\frac{\partial Z}{\partial \theta}; \quad v = \frac{g}{fR\cos\theta}\frac{\partial Z}{\partial \lambda} \tag{1}$$

where λ is longitude and θ is latitude. The Coriolis parameter f is chosen for latitude 77.5 °N.

Wind speeds u and v are the westerly and southerly components of the geostrophic flow. We calculated geopotential gradients from the estimation of a second-order centered difference, following the method of Jenkinson and Collison (1977) (cited from Losleben *et al.*, 2000). This uses three-point weighted averages of the surface heights in a 3×3 neighborhood of cells centered on the site.

The 500-mb wind vector can be constructed from the wind-speed components, giving total flow strength $F = (u^2 + v^2)^{0.5}$ and flow direction $\gamma = \tan^{-1}(v/u)$, with appropriate logic to determine the correct quadrant of the wind vector. The flow indices u, v, F, and γ were calculated for each day in the 1950–2003 NCEP fields. In addition, we calculated the vertical component of relative vorticity for each day (Gill, 1982, p. 191),

$$\xi = \frac{g}{f}\left[\frac{1}{R^2\cos^2\theta}\left(\frac{\partial^2 Z}{\partial \lambda^2}\right) + \frac{1}{R^2}\left(\frac{\partial^2 Z}{\partial \theta^2}\right)\right] \tag{2}$$

Relative vorticity ξ is an index for the strength of cyclonic or anticyclonic activity, and is negative for anticyclonic flow. It was calculated over the icefield using centered differences in a 5×5 neighborhood of cells, providing a relatively large-scale measure of ridge and trough structure and transient cyclonic activity in the region.

5.2. *Mean flow conditions in the region*

The daily flow parameters u, v, F, γ, and ξ were normally distributed for the 54-year NCEP Reanalysis period, with mean annual zonal and meridional flow close to 0 ($\overline{u} = 0.3$ m/s and $\overline{v} = 0.6$ m/s) owing to the influence of air masses from all directions in the region. Seasonal cycles are evident in flow strength, F, and 500-mb height, Z, driven by the increased strength and southward extent of the polar vortex in winter (*cf* Alt, 1987; Serreze, 1995). Cyclonic flows are predominant over the icefield, with a mean annual relative vorticity of $\overline{\xi} = 4.3 \times 10^{-5}$ s^{-1}, and with cyclonic circulation present on 62% of days in the 54-year NCEP data set. Peak cyclonic activity is in the winter and spring, with an average vorticity of 5.6×10^{-5} s^{-1} for the period December–April. Summer months are characterized by weakened cyclonic strength and increased frequency of anticyclonic systems ($\overline{\xi}_{\mathrm{JJA}} = 2.3 \times 10^{-5}$ s^{-1}) as the winter vortex weakens over the region and high-pressure ridges penetrate intermittently to the latitude of the Queen Elizabeth Islands (e.g. Bradley and England, 1979; Alt, 1978, 1987).

5.3. *Synoptic conditions, 2001–2003*

Mean daily 500-mb flow characteristics for the 2-year observation period, 2001–2003, did not deviate significantly from the long-term means, although anticyclonic and southerly flow were slightly stronger and more frequent during this time. Cyclonic vorticity prevailed over the icefield on 60% of days, close to the 54-year average, although there are significant differences between 2001–2002 and 2002–2003. In particular, summer (JJA) 2001 was characterized by a high frequency of anticyclonic circulation, 64.1% of days, while anticyclonic circulation occurred on only 38.0% of days in summer 2002 (JJA). This difference may underlie an important contrast in mean lapse rates observed in the two summers (Table III). We shall return to this difference in the analysis of summer melt from the icefield in Section 6.

To investigate the extent to which the synoptic conditions govern temperature patterns on the icefield, we analyzed daily 500-mb flow indices in conjunction with mean daily lapse rates from May 2001 to April 2003. Figure 5 plots daily lapse rates and synoptic variables for the 2-year period, giving an example of the high variability in the 500-mb flow (Figure 5(b), (d), (f)). A reconstruction of daily average temperature at the summit altitude of the icefield (1730 m) is plotted in Figure 5(c), while Figure 5(e) depicts 500-mb heights

Copyright © 2006 Royal Meteorological Society

DOI: 10.1002/joc

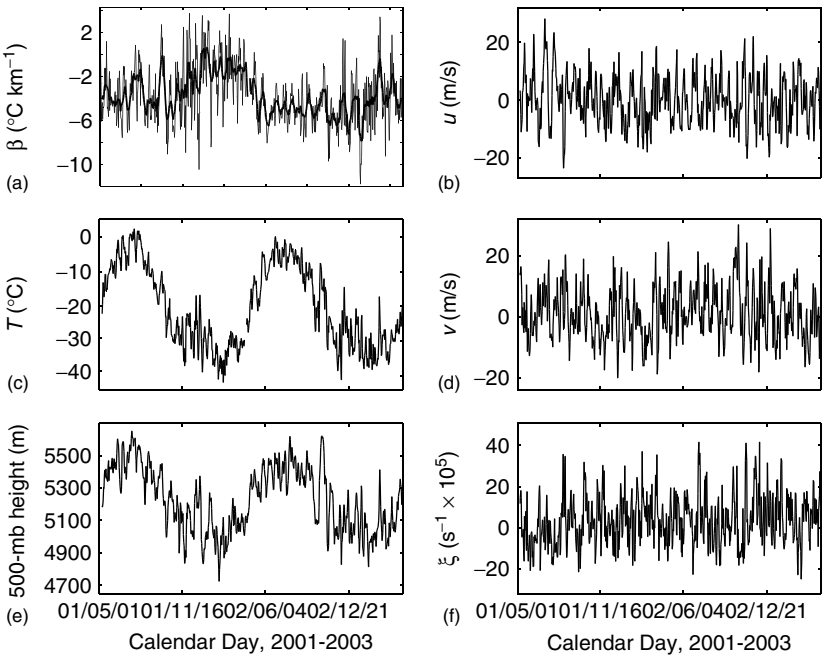

Figure 5. Daily synoptic and surface variables for the 2-year period of observation on the Prince of Wales Icefield, May 2001–April 2003. (a) Surface-temperature lapse rate, β (°C km^{-1}). (b) 500-mb westerly wind strength, u (m s^{-1}). (c) Mean daily air temperature at the Summit elevation (°C), derived from an average of all available temperature observations on the icefield and lapsed to this elevation using the daily lapse rate in (a). (d) 500-mb southerly wind strength, v (m s^{-1}). (e) 500-mb geopotential height, Z (m). (f) 500-mb vorticity, ξ (s$^{-1} \times 10^5$)

over the icefield. Visually and statistically, there is no clear relationship between daily lapse rates and synoptic conditions over the entire data set.

However, monthly analyses of the lapse rate and synoptic variability do show some recurrent patterns. To analyze these patterns further, we constructed time series of temperature and pressure anomalies as the annual cycle in each variable, evident in Figure 5(c) and (e), which dominates the daily deviations of interest. Daily anomalies were derived by subtracting the mean monthly temperature and pressure from the daily values, e.g. $\Delta T_{\mathrm{d}}(t) = T_{\mathrm{d}}(t) - \overline{T}_m$, effectively removing the seasonal cycle in each variable. We also compiled a composite relative humidity time series for the icefield on the basis of the average measurements from five sites (Figure 2).

Monthly correlations of lapse rates and several meteorological variables of interest are presented in Figure 6. We can generalize these relationships for two main seasons, the 'warm season' of June–November and the 'cold season' of December–May (Table IV). Periods with steep lapse rates in the summer and autumn correspond with high relative vorticity (strong cyclonic circulation) and low-pressure anomalies, while weak lapse rates and inversions correlate with high-pressures and anticyclonic curvature. There is also a weak correlation between steep lapse rates and southerly flow in the warm season. In contrast, relative vorticity, pressure, and southerly flow have little influence on lapse rates in the winter and spring months. Air temperature anomalies have the strongest bearing on lapse-rate strength in the cold season, with weak lapse rates and inversions associated with anomalously cold temperatures. Lapse rates have no apparent relationship with westerly flow in any season.

To examine these relationships further, we analyzed the synoptic conditions during incidences of strong ($\beta < -6\,^{\circ}$C km^{-1}) and weak ($\beta > -2\,^{\circ}$C km^{-1}) lapse rates on the icefield. For the warm season, there were 78 days with strong lapse rates and 48 days with weak lapse rates over the two years of observations. The statistics for each subset of data are compiled in Table IV. For the combined 2001 and 2002 months of June–November, the mean 500-mb height anomaly for days with steep lapse rates was −42 m, compared

Copyright © 2006 Royal Meteorological Society

DOI: 10.1002/joc

Table IV. Relationship between warm-season (June to November) and cold-season (December to May) lapse rates and synoptic weather variables, 2001–2003. The first two lines show the linear correlation between daily lapse rates and synoptic indices. The next four lines show mean 500-mb and icefield meteorological conditions for days with strong and weak lapse rates

	Westerly flow, u	Southerly flow, v	Flow F	Vorticity ξ	ΔT	ΔZ_{500}	RH
June–November	−0.05	−0.19	−0.21	−0.42	0.02	0.47	−0.13
December–May	−0.12	−0.06	0.15	−0.11	−0.31	−0.04	−0.12
June–November							
$\beta < -6\,^{\circ}\mathrm{C\ km^{-1}}$	+2.3 m s^{-1}	+2.3 m s^{-1}	11.5 m s^{-1}	9.8×10^{-5} s^{-1}	−0.84 °C	−42 m	90%
$\beta > -2\,^{\circ}\mathrm{C\ km^{-1}}$	+0.8 m s^{-1}	−1.3 m s^{-1}	9.4 m s^{-1}	-6.2×10^{-5} s^{-1}	−0.27 °C	+51 m	75%
December–May							
$\beta < -6\,^{\circ}\mathrm{C\ km^{-1}}$	+0.9 m s^{-1}	−0.0 m s^{-1}	9.4 m s^{-1}	6.8×10^{-5} s^{-1}	0.08 °C	+10 m	85%
$\beta > -2\,^{\circ}\mathrm{C\ km^{-1}}$	−2.2 m s^{-1}	−0.6 m s^{-1}	11.8 m s^{-1}	3.2×10^{-5} s^{-1}	−1.69 °C	+1 m	84%

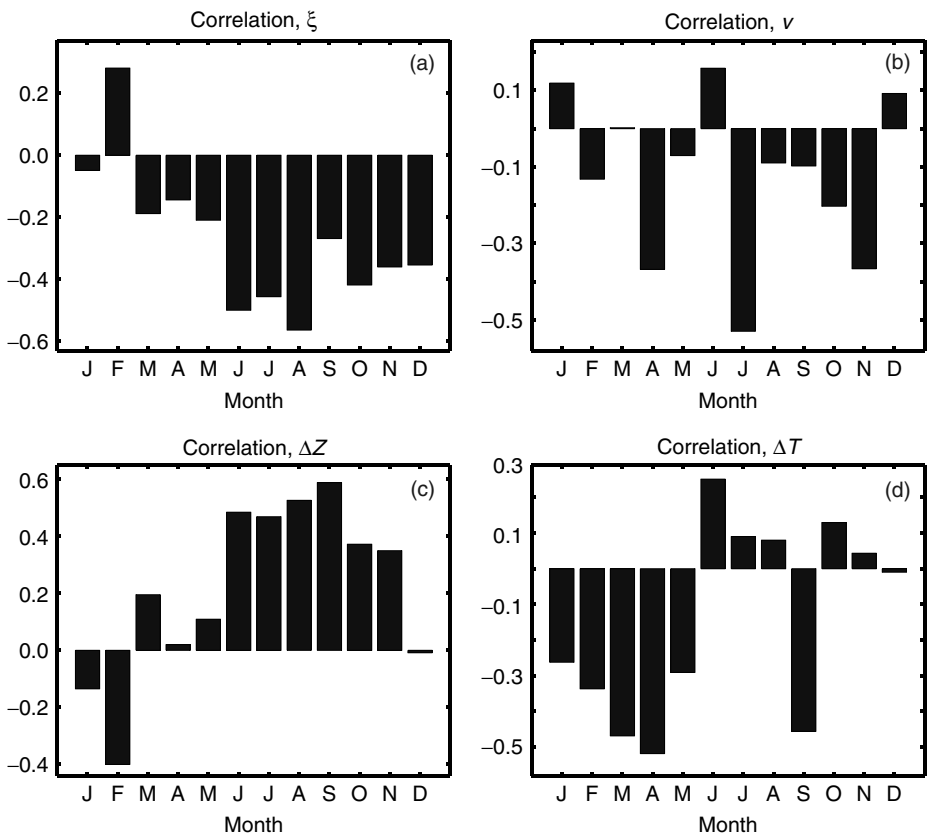

Figure 6. Monthly correlation coefficients for daily lapse rates and (a) relative vorticity, (b) southerly wind strength, (c) 500-mb height anomalies, and (d) temperature anomalies. Steep lapse rates are more negative, so a negative correlation indicates that steep lapse rates (high elevation–temperature gradients) are associated with large positive values of the variable

with +51 m for the group of days with $\beta > -2\,^{\circ}\mathrm{C\ km^{-1}}$. Low-pressure anomalies and cyclonic circulation prevailed for 73% and 77% of the days with steep lapse rates, respectively. In contrast, high-pressure and anticyclonic circulation were found for 85% and 77% of the days when lapse rates were weak. Steep warm-season lapse rates were also associated with strong southwesterly flow. Days with weak lapse rates had a

Copyright © 2006 Royal Meteorological Society

DOI: 10.1002/joc

higher frequency of northerly flows and were characterized by a low relative humidity of 75% compared with an average warm-season relative humidity of 89% on the icefield.

Table IV also presents the corresponding relationships for winter and spring months. The two years of observation give a combined count of 126 days with weak lapse rates and 52 days with steep lapse rates. The warm-season correlations generally break down during this period, with relative humidity, vorticity, and pressure anomalies having little bearing on the strength of the lapse rates. Weak lapse rates have an association with northeasterly flow. Overall, the only strong meteorological indicator of cold-season lapse rates is the daily temperature anomaly. Weak lapse rates and inversions are associated with anomalously cold intervals ($\Delta T = -1.7\,^{\circ}$C).

6. APPLICATION TO SNOWMELT MODELLING

We examined the patterns of summer snowmelt on the Prince of Wales Icefield in 2001 and 2002 as a way to illustrate the importance of the low screen-temperature lapse rates that were observed. Figure 7 plots the screen temperature and observations at the snow surface height from the POW summit site for the two summers (JJA). Table V summarizes the temperature and snowmelt data for the two summers, as well as several other synoptic and regional meteorological variables of interest.

The summer of 2001 was significantly warmer than that of 2002 on the icefield, particularly at higher altitudes. As seen in Table V, the average temperature at the summit site in JJA 2001 was $-4.2\,^{\circ}$C, with a

Table V. Temperature and snowmelt observations at the POW Summit site, summer 2001 *versus* summer 2002, along with regional and synoptic meteorological observations from each season

	POW Icefield observations						Eureka[a]	Relative vorticity
	T_{JJA} (°C)	T_{max} (°C)	PDD (°C d)	Total melt (mm w.eq.)	$\overline{\beta}_{JJA}$ (°C km^{-1})	$\overline{T}_{JJA}$ (°C)	$\xi > 0$[b] (%)	$\overline{\xi}_{JJA}$ (s$^{-1} \times 10^5$)
JJA 2001	−4.2	2.3	25.0	90	−3.7	3.8	35.9	−2.04
JJA 2002	−6.0	−1.0	1.0	0	−5.0	4.6	62.0	3.95

[a] Eureka, Nunavut (Environment Canada, 2003).
[b] Frequency of days with cyclonic circulation over the icefield.

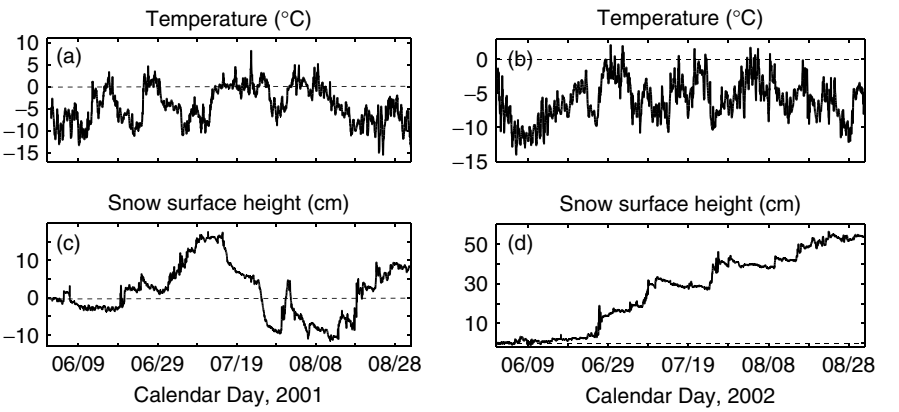

Figure 7. Summer (JJA) screen temperature and snow surface height at the POW Summit site in 2001 and 2002. (a), (b) Temperature (°C), 2001 and 2002. (c), (d) Snow surface (cm), 2001 and 2002, as measured by the SR50 ultrasonic depth gauge. The dashed lines in (a) and (b) denote 0 °C. The dashed lines in (c) and (d) correspond to the June 1 snow surface height from each year, arbitrarily assigned to be 0 cm

Copyright © 2006 Royal Meteorological Society

DOI: 10.1002/joc

maximum daily average temperature of 2.3 °C. This induced extensive melt at the summit site; on the basis of snow-density measurements and the snow surface height (SR50) data, we estimate the total melt in summer 2001 to have been 90 mm water equivalent (mm w.eq.). This is in contrast with the 0 melt at the summit site in 2002 summer when the average summer temperatures were 2.2 °C cooler and the maximum daily average temperature was −1.0 °C. Temperatures peaked above 0 °C on two occasions in summer 2002, but the heat was insufficient to warm the snow to melting point. Indeed, substantial quantities of snow accumulated through summer 2002: *ca* 51 cm or 130 mm w.eq (Figure 7(d)). These observations are consistent with snowpit studies and a 20-m ice core collected at the summit site, which indicate that melting at this location occurs only in warm years.

This amount of snowmelt or accumulation (on the order of 100 mm w.eq.) is significant for the icefield, as 40-year mean accumulation rates at the summit site are estimated to be 360 mm w.eq. (unpublished data). The observation of substantial melt in the summer of 2001 *versus* no melt in the summer of 2002 is of great importance for estimating the annual mass balance of the icefield and for the interpretation of further ice cores being collected from the site. Though interannual variability of this nature is expected, the observations come as a surprise because the Greenland Ice Sheet experienced unprecedented melt in 2002 (Steffen *et al*., 2004). The two nearest Environment Canada weather stations to our study site, in Eureka and Grise Fiord, both experienced warmer summers in 2002 than in 2001 (Environment Canada, 2003; Table V). Both of these are coastal, low-altitude sites. On the basis of these records, one would expect the icefield to have experienced extensive snowmelt in 2002, but the opposite was observed.

This can only be understood through the systematic variations in temperature lapse rates that we observed in the two summers. The average lapse rate in JJA 2001 was $-3.7\,^{\circ}\mathrm{C\ km^{-1}}$, compared with $-5.0\,^{\circ}\mathrm{C\ km^{-1}}$ in JJA 2002. This difference was large enough to create a reversal in the temperature anomaly *versus* altitude; 2002 was warmer than 2001 at coastal sites (i.e. Eureka, Grise Fiord) but colder than 2001 at altitudes above *ca* 800 m. While we do not fully understand the meteorological causes of this reversal, the observations are consistent with the prevailing synoptic conditions from each summer. Anticyclonic flow predominated over the icefield in JJA 2001 (64.1% of days) but was infrequent in JJA 2002 (38.0% of days). As discussed in Section 4, the observed lapse-rate variability can be largely attributed to this difference in relative vorticity over the icefield.

7. DISCUSSION AND CONCLUSIONS

Our analysis reveals considerable daily and seasonal variability in screen-temperature lapse rates. The overall pattern of daily lapse-rate variability was coherent on the eastern and western slopes, as well as the northern *versus* southern transects. We therefore conclude that the observed variability is regional in scale and is unlikely to be an artefact of local effects such as cold air drainage in one part of the icefield. This is supported by the results of Wang *et al*. (2005), who present a 5-year record of satellite-inferred melt season duration on a larger region in the Canadian Arctic, including our study area. Wang *et al*. find that the screen-temperature lapse-rate variability and the dichotomy between temperatures at high- and low-altitude sites are persistent features over the whole of the Canadian Arctic archipelago.

Daily lapse-rate variations do not correlate simply with any synoptic-scale or surface meteorological variable that we analyzed for the entire data set. However, significant relationships emerged when the data was separated into two groups, June–November and December–May. Specifically, summer and autumn lapse rates are steep when strong cyclonic circulation is present over the icefield, which is associated with low pressures and southerly flow at the 500-mb height. Boundary-layer temperature inversions and weak lapse rates are associated with anticyclonic systems in the region in the summer and fall, typically coinciding with positive 500-mb height anomalies. These relationships break down in winter and spring months, with no correlation between December to May lapse rates and either vorticity or 500-mb height anomalies. In contrast with summer and autumn, weak near-surface temperature gradients in winter and spring are associated with anomalously cool temperatures on the icefield.

We believe that the observed lapse-rate variability is systematic rather than stochastic, on the basis of the strength and the consistency of the correlations between lapse rates and synoptic variables. Local energy

Copyright © 2006 Royal Meteorological Society

DOI: 10.1002/joc

balance conditions appear to respond consistently to the synoptic-scale forcing to create strong but potentially predictable variability. We do not yet understand the causal relationships between the synoptic conditions and the terms of energy balance that dictate screen temperatures. In the absence of energy balance measurements from several locations on the icefield, we can only speculate on the controls of the observed lapse-rate variability. A network of AWSs spanning the full range of elevation on the icefield would allow a full energy balance assessment at different altitudes and provide a direct examination of the boundary-layer processes that underlie the lapse-rate variability.

The seasonal division that emerges from the data, June–November and December–May, corresponds with the seasonality of open-water conditions in the eastern Canadian Arctic. Open water in Baffin Bay, Davis Strait, and the inter-island channels in the summer and autumn provides a low-albedo surface and a supply of latent and sensible heat. Combined with available solar energy, this generates warmer sea-level temperatures in the summer and autumn and this may support the steeper lapse rates that are observed in these months. Cyclonic flow that is associated with low pressures over the icefield may play a role in strengthening the surface-level southeasterly flow that draws this heat and moisture inland from Baffin Bay, and promoting orographic uplift and near-surface temperature gradients that are similar to moist adiabatic lapse rates.

Cold-season lapse rates in the lower elevation range of the icefield are surprisingly steep, given the pervasive low-level free-air inversions that are present in the polar winter in the absence of solar radiative input. This likely reflects a more negative net longwave radiation balance at higher altitudes, owing to lower downwelling longwave flux (a result of clear skies and low vapour pressure). The North Water polynya in Baffin Bay is also a perennial feature (Barber *et al*., 2001) that will influence the eastern flanks of the icefield in late winter and spring. Similar to the warm season, this provides a supply of moisture and sensible heat that may contribute to low-altitude warming. The observation of steeper cold-season lapse rates on the eastern flanks of the icefield, relative to the western slopes, supports this hypothesis.

While detailed energy balance measurements are needed to better understand the synoptic meteorological controls on lapse-rate variability, it is clear that caution is required when downscaling or extrapolating boundary-layer temperatures. This is certainly the case in snowmelt modelling in hydrological or glacier mass balance studies in which snow and ice melt is commonly parameterized from cumulative positive degree days (PDD) (e.g. Huybrechts and de Wolde, 1999; Braun and Hock, 2004). Boundary-layer temperatures are typically interpolated from climate models or extrapolated from coastal/low-altitude weather records. Conventional free-air lapse rates would cause a large underestimation of melt in the interior of the icefield, while a fixed summer value of -4 to $-5\,^{\circ}\mathrm{C\ km^{-1}}$ would miss the interannual variability that was observed in 2001 and 2002. We propose that the prevailing synoptic conditions offer some predictive capability for lapse rates in our region. This means that synoptic flow indices can be combined with coastal weather data to improve models of high-altitude snow and ice melt.

Caution is warranted in applying our findings to other regions. Near-surface lapse rates are unlikely to adhere to free-air lapse rates, and they can be expected to vary in deterministic ways in all regions. However, lapse-rate magnitudes and controls will differ in different locations as a function of local energy balance regimes. Surface environment, altitude, and radiative conditions (hence, latitude) will have a large influence on this. Our observations are specific to snow/ice surfaces and may also be specific to the high-latitude environment of polar icefields. The results appear to apply to the larger region of the Canadian Arctic Archipelago (Wang *et al*., 2005), suggesting a coherent glacier mass balance feedback to shifts in synoptic conditions that may accompany climate change. This has important implications for forecasts of future sea-level rise. It remains to be seen whether the Greenland Ice Sheet is subject to similar synoptically controlled lapse-rate variability. Wang *et al*. (2005) suggest this possibility but also note that Greenland and the Canadian Arctic islands may not be synchronized. The two regions were subject to opposing geopotential height anomalies in 2002, consistent with the discrepancy in summer melt (*cf* Steffen *et al*., 2004).

We cannot comment on whether our results extend to other mountainous regions of the world, but the variability of screen-temperature lapse rates echoes those that are seen in the midlatitudes (e.g. Pepin 2000). The prevalence of low near-surface lapse rates in our observations is also consistent with reports from other regions (e.g. Humlum and Christiansen, 1998; Shea *et al*., 2004; Braun and Hock, 2004), in both glaciated and unglaciated terrain, although lapse rates of -5 to $-5.5\,^{\circ}\mathrm{C\ km^{-1}}$ appear to be more typical of unglaciated

Copyright © 2006 Royal Meteorological Society

DOI: 10.1002/joc

terrain. Diurnal lapse-rate cycles also become important at midlatitudes (Pepin and Losleben, 2002). Typical free-air values that are adopted in many studies will overestimate mean surface-temperature gradients. Multistation analyses are needed to quantify screen-temperature lapse rates for hydrological, ecological, and glaciological applications that make use of temperature downscaling in mountain regions.

ACKNOWLEDGEMENTS

We thank the Polar Continental Shelf Project of Canada, Resolute Bay, Nunavut, for essential logistical support for this study. Additional support was provided by Science and Engineering Research Canada (NSERC) grants to Marshall and Sharp, Canadian Circumpolar Institute grants to Burgess, the NSERC Climate System History and Dynamics Program, and CRYSYS. Davis Lewis and Douglas Mair provided valuable assistance in the 2002 and 2001 field seasons. We thank A. Comrie and three anonymous reviewers for their critical and thoughtful suggestions.

REFERENCES

Alt BE. 1978. Synoptic climate controls of mass balance variations on Devon Ice Cap. *Arctic and Alpine Research* **10**: 61–80.

Alt BE. 1987. Developing synoptic analogs for extreme mass balance conditions on Queen Elizabeth Island ice caps. *Journal of Climate and Applied Meteorology* **26**(12): 1605–1623.

Arnold NS, Willis IC, Sharp MJ, Richards KS, Lawson MJ. 1996. A distributed surface energy-balance model for a small valley glacier. I. Development and testing for Haut Glacier d'Arolla, Valais, Switzerland. *Journal of Glaciology* **42**(140): 77–89.

Barber DG, Hanesiak JM, Chan W, Piwowar J. 2001. Sea ice and meteorological conditions in northern Baffin Bay and the North Water Polynya between 1979 and 1996. *Atmosphere-Ocean* **39**(3): 343–359.

Bolstad PV, Swift L, Collins F, Réginiere RF. 1998. Measured and predicted air temperatures at basin to regional scales in the southern Appalachian Mountains. *Agricultural and Forest Meteorology* **91**: 161–176.

Bradley RS, England J. 1979. Synoptic climatology of the Canadian high Arctic. *Geografiska Annaler* **61A**(3–4): 187–201.

Braithwaite RJ, Olesen OB. 1989. Calculation of glacier ablation from air temperature, West Greenland. In *Glacier Fluctuations and Climatic Change*, Oerlemans J (ed.). Kluwer Academic: Dordrecht; 219–233.

Braun M, Hock R. 2004. Spatially distributed surface energy balance and ablation modelling on the ice cap of King George Island, Antarctica. *Global and Planetary Change* **42**(1–4): 45–58.

Environment Canada. 2003. Canadian climate data online. http://climate.weatheroffice.ec.gc.ca/climateData/canada_e.html.

Fyfe JC, Flato JM. 1999. Enhanced climate change and its detection over the Rocky Mountains. *Journal of Climate* **12**: 230–243.

Gill AE. 1982. *Atmosphere-Ocean Dynamics*. Academic Press: London.

Giorgi F, Hurrell JW, Marinucci MR, Beniston M. 1997. Elevation dependency of the surface climate change signal: a model study. *Journal of Climate* **10**: 288–296.

Glover RW. 1999. Influence of spatial resolution and treatment of orography on GCM estimates of the surface mass balance of the Greenland Ice Sheet. *Journal of Climate* **12**: 551–563.

Greuell W, Böhm R. 1998. 2-m temperatures along melting mid-latitude glaciers, and implications for the sensitivity of the mass balance to variations in temperature. *Journal of Glaciology* **44**(146): 9–20.

Hare FK. 1968. The Arctic. *Quarterly Journal of the Royal Meteorological Society* **94**(402): 439–459.

Humlum O, Christiansen HH. 1998. Mountain climate and periglacial phenomena in the Faroe Islands, SE North Atlantic Ocean. *Permafrost and Periglacial Processes* **9**: 189–211.

Huybrechts P, de Wolde J. 1999. The dynamic response of the Greenland and Antarctic Ice Sheets to multiple-century climate warming. *Journal of Climate* **12**: 2169–2188.

Jenkinson AF, Collison P. 1977. *An Initial Climatology of Gales Over the North Sea*, *Synoptic Climatology Branch Memorandum No. 62*. Meteorological Office: London; 18.

Jóhannesson T, Sigurdsson O, Laumann T, Kennett M. 1995. Degree-day glacier mass-balance modelling with application to glaciers in Iceland, Norway, and Greenland. *Journal of Glaciology* **41**: 345–358.

Kalnay E, Kanamitsu M, Kistler R, Collins W, Deaven D, Gandin L, Iredell M, Saha S, White G, Woollen J, Zhu Y, Leetmaa A, Reynolds B, Chelliah M, Ebisuzaki W, Higgins W, Janowiak J, Mo KC, Ropelewski C, Wang J, Jenne R, Joseph D. 1996. The NCEP/NCAR 40-year reanalysis project. *Bulletin of the American Meteorological Society* **77**: 437–471.

Legates DR, Willmott CJ. 1990. Mean seasonal and spatial variability in global surface air temperature. *Theoretical and Applied Climatology* **41**: 11–21.

Leung LR, Wigmosta MS. 1999. Potential climate change impacts on mountain watersheds in the Pacific Northwest. *Journal of the American Water Resources Association* **35**(6): 1463–1471.

Losleben M, Pepin N, Pedrick S. 2000. Relationships of precipitation chemistry, atmospheric circulation, and elevation at two sites on the Colorado Front Range. *Atmospheric Environment* **34**: 1723–1737.

McCutchan MH. 1983. Comparing temperature and humidity on a mountain slope and in the free air nearby. *Monthly Weather Review* **111**: 836–845.

McCutchan MH, Fox DG. 1986. Effect of elevation and aspect on wind, temperature, and humidity. *Journal of Climate and Applied Meteorology* **25**: 1996–2013.

Pepin N. 2000. Twentieth century change in the climate record from the Front Range, Colorado, U.S.A. *Arctic Antarctic and Alpine Research* **32**(2): 135–146.

Copyright © 2006 Royal Meteorological Society

DOI: 10.1002/joc

Pepin N, Losleben M. 2002. Climate change in the Colorado Rocky Mountains: free air versus surface temperature trends. *International Journal of Climatology* **22**: 311–329.

Pepin N, Benham D, Taylor K. 1999. Modeling lapse rates in the maritime uplands of Northern England: implications for climate change. *Arctic Antarctic and Alpine Research* **31**(2): 151–164.

Pielke RA, Mehring P. 1977. Use of mesoscale climatology in mountainous terrain to improve the spatial representation of mean monthly temperatures. *Monthly Weather Review* **105**: 108–112.

Pollard D, Thompson S. 1997. Driving a high-resolution dynamic ice-sheet model with GCM climate: ice-sheet initiation at 116,000 BP. *Annals of Glaciology* **25**: 296–304.

Reeh N. 1991. Parameterization of melt rate and surface temperature on the Greenland Ice Sheet. *Polarforschung* **59**: 113–128.

Richner H, Phillips PD. 1984. A comparison of temperature from mountaintops and form the free atmosphere – their diurnal variation and mean difference. *Monthly Weather Review* **112**: 1328–1340.

Samelson RM, Agnew T, Melling H, Münchow A. 2006. Evidence for atmospheric control of sea-ice motion through Nares Strait. *Geophysical Research Letters* **33**: L02506, Doi: 10.1029/2005GL025016.

Serreze M. 1995. Climatological aspects of cyclone development and decay in the Arctic. *Atmosphere-Ocean* **33**: 1–23.

Shea JM, Marshall SJ, Livingston JL. 2004. Glacier distributions and climate in the Canadian Rockies. *Arctic Antarctic and Alpine Research* **36**(2): 272–280.

Seidel DJ, Free M. 2003. Comparison of lower-tropospheric temperature climatologies and trends at low and high elevation radiosonde sites. *Climatic Change* **59**: 53–74.

Steffen K, Nghiem SV, Huff R, Neumann G. 2004. The melt anomaly of 2002 on the Greenland Ice Sheet from active and passive microwave satellite observations. *Geophysical Research Letters* **31**(20): L20402 Doi: 10.1029/2004GL020444.

Tabony RC. 1985. The variation of surface temperature with altitude. *Meteorological Magazine* **114**: 37–48.

Trombotto D, Buk E, Hernandez J. 1997. Monitoring of mountain permafrost in the Central Andes, Cordon del Plata, Mendoza, Argentina. *Permafrost and Periglacial Processes* **8**: 123–129.

Walland DJ, Simmonds I. 1996. Sub-grid scale topography and the simulation of Northern Hemisphere snow cover. *International Journal of Climatology* **16**: 961–982.

Wang L, Sharp M, Rivard B, Marshall S, Burgess D. 2005. Melt season duration on the Canadian Arctic ice caps, 2000–2004. *Geophysical Research Letters* **32**: L19502, Doi: 10.1029/2005GL023962.

Zuo Z, Oerlemans J. 1997. Contribution of glacier melt to sea level rise since AD 1865: a regionally differentiated calculation. *Climate Dynamics* **13**: 834–845.

Copyright © 2006 Royal Meteorological Society

DOI: 10.1002/joc